ChemPubSoc Europe

DOI: 10.1002/chem.201700883

CHEMISTRY A European Journal Full Paper

DNA Sensing

Polyadenine-Modulated DNA Conformation Monitored by Surface-Enhanced Raman Scattering (SERS) on Multibranched Gold Nanoparticles and Its Sensing Application

Jingxing Guo, Yunlong Chen, Yongjia Jiang, and Huangxian Ju*[a]

Abstract: This work proposes a facile way to modulate the conformation of DNA from the "Lie-Down" to the "Stand-Up" conformation on the surface of multibranched gold nanoparticles (AuNPs). This is realized by regulating the length of polyadenine (polyA) linked to the DNA sequence and/or the hybridization of this sequence with the target DNA, and can be monitored by the Raman signal owing to the excellent performance of multibranched AuNPs (AuNSs) as a surface-enhanced Raman scattering (SERS) substrate and the distance change between the Raman reporter and the substrate. The probable mechanism, which depends on the repulsion of polyA from the sequence and the tip assembly, has also been probed through theoretical simulation using the finite difference time domain method. By virtue of this strategy, a conformation-transformation-based DNA@AuNS sensor is constructed for the identification of a specific oligonucleotide, which has been used for the detection of DNA sequences associated with Severe Acute Respiratory Syndrome (SARS). This strategy leads to a novel sensing platform with good extendibility for DNA analysis, and provides a powerful protocol for facilitating the cognition of DNA conformation on metal surfaces.

Introduction

Au nanoparticles (AuNPs), which possess distinct physical and chemical attributes, present unique advantages in a large number of applications.[1–7] Their characters can be tuned easily by varying their size and shape. Various gold nanostructures such as nanospheres,[8–10] nanoshells,[11–13] nanorods,[14–16] multibranched AuNPs,[17–22] and bimetallic nanoparticles[23,24] have been constructed for biosensing and biomedical applications. In recent years, multibranched AuNPs, including nanoflowers,[17,18] nanostars,[19–21] and gold lace nanoshells,[22] have attracted considerable attention owing to their large surface area, sharp tips, and the presence of branches. Both theoretical calculations[25,26] and experimental measurements[27] have confirmed the occurrence of an enhanced electromagnetic field near their surface, which is beneficial for the sensitivity of optical analysis. An ultrasensitive sensor based on the surface-enhanced Raman scattering (SERS) effect of nanostars has been constructed for the detection of 1,5-naphthalenedithiol at the zeptomole level.[28] The SERS effect depends strongly on the distance between the Raman molecule and the substrate, which provides an opportunity to develop a distance-dependent methodology for different applications.

Because of their diverse structural and functional features, DNA nanostructures have been exploited as excellent biomaterials for molecular recognition and microscopic manipulations.[29] Some nanostructures have become attractive systems in biosensing applications through modulation of the DNA conformation on DNA-functionalized gold nanoparticles (DNA@AuNPs) to change the catalytic activity,[30] and distance-dependent signals, including color,[31,32] fluorescence resonant energy transfer,[32,33] and SERS.[34,35] A dynamic light scattering method has also been developed to study the conformation evolution of DNA on relatively uniform spherical AuNPs.[36] However, the difficulty in modulating the DNA status and conformation on rough surfaces[37,38] leads to a lack of modulation and sensing methodologies based on multibranched AuNPs, though several SERS-based DNA hybridization detection methods with monotonously flat Au surfaces have been developed.[39–41] To overcome this difficulty, in this work we used gold nanostars (AuNSs) as the model for assembling the Raman molecule (Cy5)-labeled DNA, and developed a facile way to modulate the DNA conformation, which allowed in situ SERS monitoring of the DNA conformation change.

The assembly of DNA on AuNPs can usually be performed by the binding of thiolated oligonucleotides through Au–S chemistry[33] and the intrinsic affinity of polyadenine (polyA) for the gold surface.[42,43] Moreover, the assembled polyA layer retains electrostatic and steric repulsion to the oligonucleotide, which promotes the extension of the oligonucleotide into solution.[44] Here, a series of polyA-grafted oligonucleotides were assembled on AuNSs. Through adjustment of the length of polyA, this assembly led to a convenient way to achieve the conformation transformation of DNA from the "Lie-Down" to

[a] J. Guo, Y. Chen, Y. Jiang, Prof. Dr. H. Ju
State Key Laboratory of Analytical Chemistry for Life Science
School of Chemistry & Chemical Engineering, Nanjing University
Nanjing 210023 (P. R. China)
E-mail: hxju@nju.edu.cn

Supporting information for this article can be found under: https://doi.org/10.1002/chem.201700883.

the "Stand-Up" conformation on the AuNS surface (Scheme 1, left). Clearly, the transformation changed the distance between another DNA end and the AuNS surface. Thus, a methodology could be produced by labeling the end with a Raman molecule

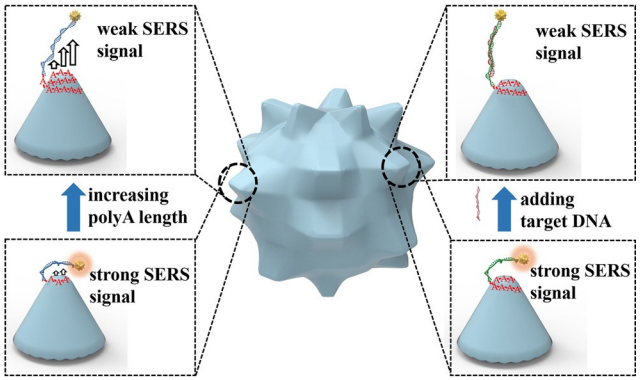

Scheme 1. Schematic illustration of DNA conformation modulation with polyA length on AuNS and in situ SERS monitoring of conformation transformation.

for in situ SERS monitoring of the conformation transformation. As a proof of concept, a Cy5-labeled polyA-grafted oligonucleotide was used as the probe to be assembled on the AuNS. The recognition of the probe for the target DNA produced a clear decrease in the SERS signal (Scheme 1, right), which led to a distance-dependent SERS methodology for both biosensing and in situ monitoring of DNA conformation. Unlike previous SERS-based DNA hybridization detection methods,[39,41] this strategy could be performed in one step, indicating its potential applications in both biosensing and in situ monitoring of DNA conformation.

Results and Discussion

AuNSs were synthesized according to the method described in a previous report.[45] The TEM image of the AuNSs shows their uniformity (Figure 1 A) with a core radius of 30.2 ± 3.0 nm (Figure S1 A, Supporting Information) and numerous sharp tips (Figure 1 A, inset). The tip radius of curvature was measured to be 2.95 ± 0.63 nm (Figure S1 B, Supporting Information). As expected, the AuNSs exhibited a very rough surface (Figure S2, Supporting Information). The UV/Vis spectrum showed well-defined localized surface plasmon features with an intense absorbance band centered at 662 nm upon dispersion in buffer solution (Figure 1 B).

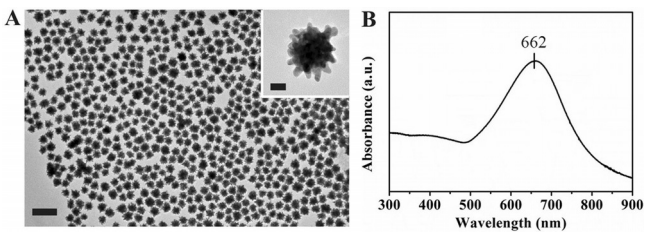

Figure 1. A) TEM image of AuNS (scale bar: 200 nm). Inset: magnified image of single AuNS (scale bar: 20 nm). B) UV/Vis spectrum of AuNS.

For realization of the "Lie-Down-to-Stand-Up" DNA conformation change by modulating the polyA length, an oligonucleotide sequence containing 26 bases (P1) labeled with Raman reporter Cy5 at the 3′ end was grafted with seven different lengths of polyA as the tail at the 5′ end (A5-P1, A10-P1, A20-P1, A30-P1, A40-P1, A50-P1, and A60-P1), respectively. After these Cy5-labeled oligonucleotides were assembled on the AuNS surface, the SERS spectra of the formed ssDNA@AuNS showed distinct Raman peaks at 932, 1121, 1215, 1264, 1362, 1404, 1467, 1496, and 1595 cm^{-1} (Figure 2 A),

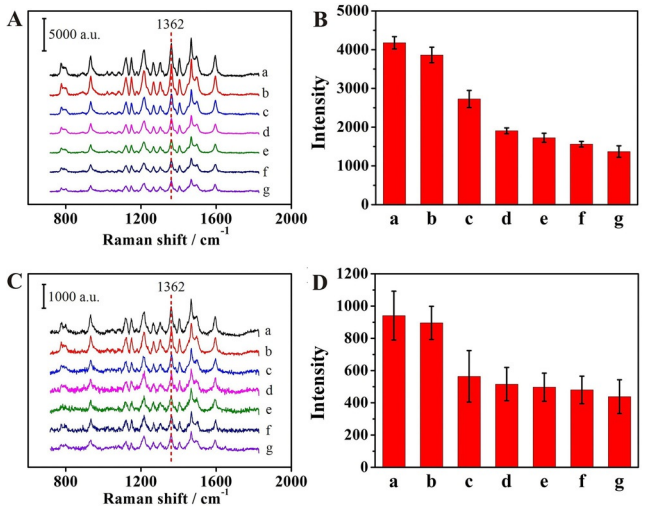

Figure 2. A, C) SERS spectra with exposure time of 1 s and 100 % laser power under 633 nm after baseline subtraction, and B, D) peak intensities at 1362 cm^{-1} for ssDNA@AuNS (A, B) and dsDNA@AuNS (C, D) with different lengths of polyA: a) A5, b) A10, c) A20, d) A30, e) A40, f) A50, and g) A60. Each spectrum in (A, C) and peak intensity in (B, D) is the mean of ten measurements.

which did not occur for AuNS (Figure S3, Supporting Information). These Raman peaks should originate from Cy5. The Raman peak at 1362 cm^{-1} could be assigned to the methine chain deformation of Cy5,[39,46] and the peaks at 1215 and 1595 cm^{-1} were assigned to ν(C=C) (benzene) and ν_{sy}(C–C) (benzene ring) in Cy5, respectively.[47] The peak intensity at 1362 cm^{-1} decayed rapidly from A5 to A30, and then tended to a steady value (Figure 2 B). The peak intensities at 1215 and 1595 cm^{-1} showed a similar variation tendency (Figure S4 A,B, Supporting Information). The SERS response is highly distance-dependent, so these results indicate the conformation change of the assembled DNA from the "Lie-Down" to the "Stand-Up" conformation with increasing polyA length. This phenomenon could be attributed to the electrostatic and steric repulsion of polyA and P1.[44] After these grafted P1 were hybridized with the sequence complementary to P1, the formed double-stranded sequences were also assembled on AuNSs to observe the change in SERS signal. The SERS spectra of the dsDNA@AuNS conjugates showed similar variation of the Cy5 SERS peaks, but their peak intensities were much weaker than those of the corresponding ssDNA@AuNS (Figure 2 C, D and Figure S4 C, D,

Supporting Information), indicating the dually increasing distance between Cy5 and the AuNS surface owing to the repulsion of polyA to P1 and the formed double-stranded structure for the conformation change from "Lie-Down" to "Stand-Up".

For demonstration of the dependence of the SERS variation on the DNA conformation transformation on the substrate surface, two factors that may affect the SERS signal, that is, substrate morphology and Cy5 concentration on the substrate, should be excluded. First, the substrate morphology of ssDNA@AuNS and dsDNA@AuNS conjugates was characterized by TEM (Figure S5, Supporting Information). Even though the radius of curvature is slightly annealed (3.37 ± 0.58 nm, Figure S6), these conjugates maintained the same characteristic multibranched structures of AuNS, which means that the polyA length and DNA conformation transformation did not change the AuNS morphology significantly. The surface density of Cy5 on the conjugates could be quantified by using a displacement-based fluorescence method;[48] this did not show any statistically significant change (< ± 10%) upon increasing the length from A5 to A40 on both ssDNA@AuNS and dsDNA@AuNS (Figure 3A). Compared with A10-P1@AuNS, the

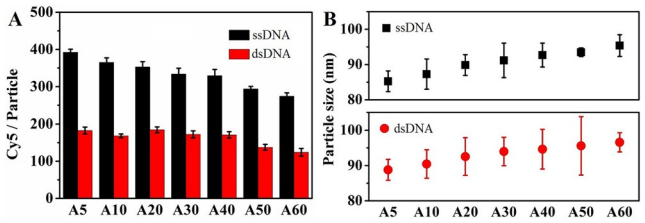

Figure 3. A) Amounts of Cy5 on DNA@AuNS surfaces and B) hydrodynamic diameters of DNA@AuNS with different lengths of polyA.

SERS intensity of ssA20-P1@AuNS and dsA20-P1@AuNS decreased by 29.4 and 29.2%, respectively, whereas the amount of Cy5 changed by only 3.3 and −9.7%, respectively. At A20, further increasing the polyA length led to a similar change in SERS intensity (by 30.0% from A20-P1 to A30-P1), and the amount of Cy5 changed by 5.4%. Thus, the decrease in the SERS signal is attributed mainly to the conformation change, which increased the distance from Cy5 to the AuNS surface. For further verification of this deduction, the sizes of the DNA@AuNS conjugates were examined through dynamic light scattering (DLS) measurements. The mean hydrodynamic diameters of both ssDNA@AuNS and dsDNA@AuNS conjugates increased and gradually levelled off with increasing polyA length (Figure 3B), indicating the extending of P1 away from the surface. The peak position (λ_{max}) of the localized surface plasmon resonance (LSPR) spectrum can be used to assess the effective layer thickness on the nanoparticle surface.[49] As expected, the λ_{max} value of ss/dsDNA@AuNS shifted to longer wavelengths with increasing polyA length (Figure S7, Supporting Information).

The amounts of Cy5 on dsDNA@AuNS were almost half those on ssDNA@AuNS (Figure 3A). However, the SERS signals were 3.5–5.5 times those of dsA20-P1@AuNS. This phenomenon can also be attributed to the further increase in conjugate size (Figure 3B) or the distance between Cy5 and the substrate surface upon hybridization. Compared with ssDNA, dsDNA adopted a more extended conformation at the AuNS surface. The similar tendency of the change in SERS signal with the size or distance suggests that SERS is a powerful tool for monitoring DNA conformation transformation on metal surfaces.

For a better understanding of the modulation process of DNA conformation on the AuNS surface by regulating the polyA length, the EM field distribution of the single DNA@AuNS nanostructure in an aqueous environment was analyzed through the finite-difference time domain (FDTD) method.[50] An enhancement of the Raman cross-section is proportional to the fourth power of the field enhancement ($|E|^4$), so it is clear that the Raman "hot spots" are located almost at the tips of branches under 633 nm excitation (Figure S8, Supporting Information). Thus, it could be speculated that the DNA conformation transformation revealed by SERS probably occurs in the tip area. Owing to the nanoscale radius curvature, the tip area of branches in AuNS possesses high surface energy for the attachment of polyA, and the tip is more exposed to the surroundings, making polyA easy to reach. Thus, the experimental results showed different phenomena from those reported on spherical gold nanoparticles.[30,45] Upon increasing the polyA length, the number of adenine deoxynucleotides (dA) at the tip area of the DNA@AuNS conjugates increased and then tended to the maximum values (Figure S9, Supporting Information), indicating that polyA-based sequences are more likely to be attached on this area than other regions to achieve the tip assembly. With increasing dA number, the electrostatic and steric repulsion from the dA layer is gradually enhanced, leading to the DNA conformation transformation from "Lie-Down" to "Stand-Up". Owing to its duplex structure, dsDNA suffered more repulsion from polyA. Both the repulsion and the rigid structure of dsDNA contribute to its preference for a relatively upright conformation.

For verification of the modulation mechanism, thiolated P1 (P1-SH) and its double-stranded structure were designed to be assembled on AuNS. These showed similar SERS signals (Figure S10, Supporting Information), indicating a similar distance between the labeled Cy5 and the Au substrate. This could be attributed to the complete coverage of thiolated probes on the AuNS surface through Au–S bonds and the presence of the multibranches, which meant that the formation of the double-stranded rigid structure did not change the average distance between Cy5 and the Au surface. Thus, both the repulsion from polyA and the tip assembly of the probe on the AuNS played important roles in the transformation from the "Lie-Down" conformation.

The DNA-conformation-dependent SERS signal could be used for sensitive identification of the formation of a double-stranded structure by hybridization of the polyA grafted probe with its target. Using a sequence associated with Severe Acute Respiratory Syndrome (SARS) as the model target, its probe (P2) was first grafted with polyA of different lengths. Upon hybridization, the decrease in SERS signal showed a maximum value at A20 (Figure S11, Supporting Information). Therefore, A20-P2 was used for preparation of the sensor by assembling

it on the AuNS. The SERS intensity of Cy5 decreased with increasing target (T) concentration, and the peak intensity at 1362 cm^{-1} was logarithmically proportional to the concentration from 0.1 to 500 nM with a detection limit of 45.7 pM (Figure 4A,B). Furthermore, after incubation of the sensor with

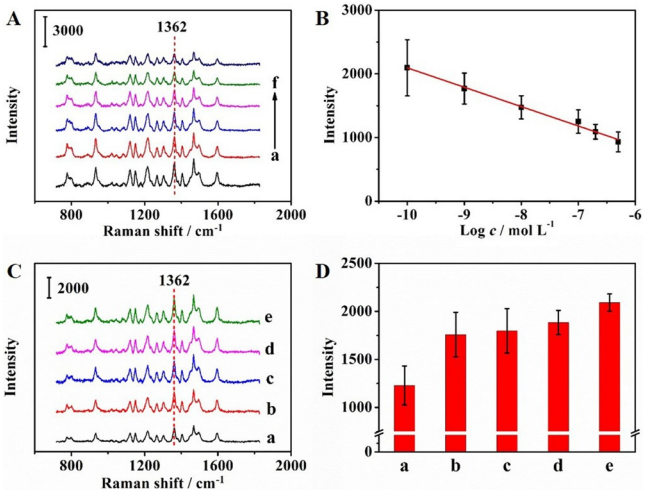

Figure 4. SERS spectra of A20-P2@AuNS sensor with exposure time of 1 s and 100% laser power under 633 nm after baseline subtraction in response to A,B) 0.1, 1.0, 10, 100, 200, and 500 nM target DNA (a–f), C,D) a) T, b) smT, c) tmT, d) nT (non-complementary T) at 50 nM, and e) blank. B,D) Mean peak intensities are measured at 1362 cm^{-1} five times to "Stand-Up" conformation.

50 nM T, single-base mismatched T (smT), and three-base mismatched T (tmT) for 6 h, the target presented a decrease in SERS signal of 41.3% at 1362 cm^{-1}, and smT and tmT showed a decrease of 15.9 and 14.1%, respectively (Figure 4C,D), indicating the more upright conformation of the double-stranded structure and the excellent selectivity of the SERS sensor for DNA detection. Furthermore, after storage of the sensor at 4 °C for one week, a signal change of less than 6% was measured, indicating acceptable stability.

Conclusion

In this work we have developed a facile method for the modulation of DNA conformation from the "Lie-Down" to the "Stand-Up" conformation on a AuNS surface by adjusting the length of tip-assembled polyA grafted to the DNA sequence. The process of conformation transformation can be monitored precisely in situ by the SERS signal. Moreover, the in situ SERS monitoring methodology can be employed to identify target DNA from mismatched sequences with good sensitivity and selectivity through their conformation change after hybridization. This strategy can be extended for the design of new distance-dependent sensing methodologies with multibranched nanoparticles, and provides a powerful tool for the study of DNA conformation.

Experimental Section

Materials and reagents

Ethanol, *N*,*N*-dimethylformamide (DMF), ethylenediamine tetraacetic acid (EDTA), trisodium citrate, and hydrochloric acid (HCl) were obtained from Sinopharm Chemical Reagent Co., Ltd (China). Chloroauric acid ($HAuCl_4 \cdot 3H_2O$), β-mercaptoethanol, tris (hydroxymethyl) amino-methane, tris (2-carboxyethyl) phosphine hydrochloride solution (0.5 M, pH 7.0) (TCEP), and polyvinylpyrrolidone (PVP) were purchased from Sigma–Aldrich Inc. (USA). Tris-EDTA buffer containing 10 mM Tris-HCl and 1 mM EDTA (TE, pH 7.40, containing 0.005% Tween-20) was used as reaction buffer. All other reagents were of analytical grade. All aqueous solutions were prepared using ultrapure water (18 MΩ, Milli-Q, Millipore). All oligonucleotides used in this work were purchased from Sangon Biological Engineering Technology & Co. Ltd. (Shanghai, China). Their sequences are displayed in Table S1, Supporting Information.

Apparatus

Raman spectra were recorded on a Renishaw InVia confocal Raman microscope (Renishaw, UK) using 633 nm excitation with 100% laser power. A 50× telephoto objective was used for observation and spectral measurements. The transmission electron microscopic (TEM) and scanning electron microscopic (SEM) images were gained on a JEM-2100 transmission electron microscope (JEOL Ltd., Japan) and S-4800 scanning electron microscope (HITACHI, Japan), respectively. The TEM images were analyzed by Image J software to estimate the core size and the tip radius of curvature. Dynamic light scattering (DLS) was performed on 90 Plus/BI-MAS equipment (Brookhaven, USA). The localized surface plasmon resonance (LSPR) absorption spectra were recorded on a UV-3600 UV/Vis/NIR spectrophotometer (SHIMADZU, Japan), and the fluorescence experiments were performed on F-7000 fluorescence spectrophotometer (HITACHI, Japan).

Synthesis of gold nanostars (AuNSs)

The synthesis of AuNSs was based on a previous report.[45] In brief, the 15 nm PVP-coated Au seeds were prepared by adding trisodium citrate (5 mL, 1 wt%) into boiling $HAuCl_4$ solution (100 mL, 0.5 mM) and cooling to room temperature. PVP (8.6 mL, 25.6 $g L^{-1}$, $M_W = 10\,000$) was added dropwise and the mixture was allowed to stand overnight. The obtained Au seeds were rinsed with ethanol by centrifugation (4000 rpm, 90 min) and dispersed in ethanol. The concentration of the dispersion was determined by using UV/Vis absorption spectrometry.[51] The AuNSs were synthesized by adding ethanol solution (43 μL) of Au seeds (4.2 mM) into a DMF solution (15 mL) of $HAuCl_4$ (0.3 mM) and PVP (10 mM) under rapid stirring at room temperature. The resulting AuNSs were washed three times by centrifugation (6000 rpm, 10 min) and redispersed in ethanol.

Preparation of DNA@AuNS conjugates

The as-prepared AuNSs (1 nM, concentrated in 1×TE buffer) were sonicated for 1 h and then mixed with polyA-based DNA (A5-P1, A5-P2, A10-P1, A10-P2, A20-P1, A20-P2, A30-P1, A30-P2, A40-P1, A40-P2, A50-P1, A50-P2, A60-P1, A60-P2, and their hybridized dsDNA) for 16 h at 37 °C. The mixtures were brought to 1×TE buffer (pH 7.4, 0.005% Tween-20) containing 0.1 M NaCl and incubated at 37 °C for 40 h. Subsequently, the obtained polyA-based DNA@AuNS conjugates were washed three times in 1×TE buffer (pH 7.4, 0.005% Tween-20) through centrifugation (6000 rpm,

10 min) to remove excess DNA, and resuspended in 1 mL 1×TE buffer (pH 7.4, 0.005% Tween-20, 0.1 M NaCl).

For the preparation of P1-SH@AuNS, P1-SH was first activated with TCEP at a DNA/TCEP molar ratio of 50:1 for 1 h, mixed with the as-prepared AuNSs (1 nM) for 16 h at 37 °C, and then added dropwise to NaCl (2 M) to a concentration of 0.05 M. The mixture was allowed to stand for 4 h, then this process was repeated thrice, and finally salted to 0.2 M NaCl. The obtained P1-SH@AuNS was washed and resuspended through a procedure similar to that for the polyA-based conjugates. The dsDNA@AuNS was prepared by activating its hybridized dsDNA through the same procedure.

For the identification of the recognition of P2 for its target SARS DNA, A20-P2 was mixed with AuNSs for 16 h at 37 °C, then brought to 1×TE buffer (pH 7.4, 0.005% Tween-20) containing 0.1 M NaCl and incubated at 37 °C for 40 h. The obtained DNA@AuNS sensor was washed and resuspended by following the same procedure as described above. Different concentrations of T and 50 nM smT, tmT, and nT were mixed with 1 mL A20-P2@AuNS, respectively, and incubated for 6 h at 37 °C to perform the Raman measurements. The blank group was made by incubating A20-P2@AuNS with TE buffer.

Raman measurements

The DNA@AuNS conjugates were dropped on a glass slide for SERS measurements. The SERS spectra of the samples were obtained by the spectral acquisition mode using the static scan type at a center wavenumber of 1300 cm^{-1} with an exposure time of 1 s and 100% laser power at 633 nm. The data were analyzed with WiRE 3.4 software.

Quantification of polyA-based DNA surface density on AuNSs

Because the amounts of polyA-based DNA and Cy5 were identical, their surface densities could be quantitated by using the protocol described by G. Viswanadham et al.[48] In brief, β-mercaptoethanol (0.88 μL, final concentration 12 mM) was added to polyA-based DNA@AuNS conjugates (1 mL) and incubated overnight with gentle shaking. Then, the AuNSs and released DNA were separated by centrifugation (6000 rpm, 10 min). The supernatant that contained the polyA-based DNA labeled by Cy5 was measured with a fluorescence spectrometer to obtain the concentration of Cy5 from a linear calibration curve, from which the surface density of polyA-based DNA on the conjugates could be obtained.

Finite-difference time domain (FDTD) simulation of DNA@AuNS structure

The FDTD simulation was performed with the commercial FDTD software package Lumerical@FDTD Solution 8.6. The DNA@AuNS structure model was 30 nm in radius and had 12 points around the core, and was referred to the TEM images (Figure S5, Supporting Information). To approach the real environment, one DNA@AuNS conjugate was located at the center of a $1(x)\times1(y)\times1\ \mu m(z)$ box that represents the water surrounding media with an index of 1.33. The simulation object had periodic boundary conditions in *y* and *z* and a PML boundary condition in *x*. A plane wave was used as the excitation source of 633 nm in wavelength propagated along the *x* axis with its polarization along the *y* direction. Note that the mesh size around the corners was 0.3 nm, and the cross-section view of the simulation region was monitored from the *XY* plane.

Acknowledgements

We gratefully acknowledge the National Natural Science Foundation of China (21635005, 21361162002, 21605080).

Conflict of interest

The authors declare no conflict of interest.

Keywords: DNA conformation modulation · DNA recognition · DNA sensing · multibranched gold nanoparticles · polyadenine · Raman spectroscopy · SERS

[1] E. Boisselier, D. Astruc, *Chem. Soc. Rev.* **2009**, *38*, 1759 – 1782.
[2] M.-C. Daniel, D. Astruc, *Chem. Rev.* **2004**, *104*, 293 – 346.
[3] R. C. Qian, L. Ding, L. W. Yan, M. F. Lin, H. X. Ju, *J. Am. Chem. Soc.* **2014**, *136*, 8205 – 8208.
[4] M. Zayats, R. Baron, I. Popov, I. Willner, *Nano Lett.* **2005**, *5*, 21 – 25.
[5] W. Zhao, M. A. Brook, Y. Li, *ChemBioChem* **2008**, *9*, 2363 – 2371.
[6] U. F. H. Bunz, V. M. Rotello, *Angew. Chem. Int. Ed.* **2010**, *49*, 3268 – 3279; *Angew. Chem.* **2010**, *122*, 3338 – 3350.
[7] R. A. Sperling, P. R. Gil, F. Zhang, M. Zanella, W. J. Parak, *Chem. Soc. Rev.* **2008**, *37*, 1896 – 1908.
[8] Y. Cheng, A. C. Samia, J. D. Meyers, I. Panagopoulos, B. W. Fei, C. Burda, *J. Am. Chem. Soc.* **2008**, *130*, 10643 – 10647.
[9] Q. Zhang, N. Iwakuma, P. Sharma, B. M. Moudgil, C. Wu, J. McNeill, H. Jiang, S. R. Grobmyer, *Nanotechnology* **2009**, *20*, 395102.
[10] P. Ghosh, G. Han, M. De, C. K. Kim, V. M. Rotello, *Adv. Drug Delivery Rev.* **2008**, *60*, 1307 – 1315.
[11] H. Wang, J. Kundu, N. J. Halas, *Angew. Chem. Int. Ed.* **2007**, *46*, 9040 – 9044; *Angew. Chem.* **2007**, *119*, 9198 – 9202.
[12] M. Ji, M. Xu, W. Zhang, Z. Yang, L. Huang, J. Liu, Y. Zhang, L. Gu, Y. Yu, W. Hao, P. An, L. Zheng, H. Zhu, J. Zhang, *Adv. Mater.* **2016**, *28*, 3094 – 3101.
[13] M. Rycenga, Z. Wang, E. Gordon, C. M. Cobley, A. G. Schwartz, C. S. Lo, Y. Xia, *Angew. Chem. Int. Ed.* **2009**, *48*, 9924 – 9927; *Angew. Chem.* **2009**, *121*, 10108 – 10111.
[14] X. Huang, S. Neretina, M. A. El-Sayed, *Adv. Mater.* **2009**, *21*, 4880 – 4910.
[15] G. von Maltzahn, A. Centrone, J. Park, R. Ramanathan, M. J. Sailor, T. A. Hatton, S. N. Bhatia, *Adv. Mater.* **2009**, *21*, 3175 – 3180.
[16] S. C. Boca, S. Astilean, *Nanotechnology* **2010**, *21*, 235601.
[17] J. Xie, Q. Zhang, J. Y. Lee, D. I. C. Wang, *ACS Nano* **2008**, *2*, 2473 – 2480.
[18] Z. He, S. Zang, Y. Liu, Y. He, H. Lei, *Biosens. Bioelectron.* **2015**, *73*, 85 – 92.
[19] S. Barbosa, A. Agrawal, L. Rodríguez-Lorenzo, I. Pastoriza-Santos, R. Alvarez-Puebla, A. Kornowski, H. Weller, L. M. Liz-Marzán, *Langmuir* **2010**, *26*, 14943 – 14950.
[20] W. Niu, Y. A. A. Chua, W. Zhang, H. Huang, X. Lu, *J. Am. Chem. Soc.* **2015**, *137*, 10460 – 10463.
[21] W. Kim, N. Kim, J. W. Park, Z. H. Kim, *Nanoscale* **2016**, *8*, 987 – 994.
[22] M. Yang, R. Alvarez-Puebla, H. S. Kim, P. Aldeanueva-Potel, L. M. Liz-Marzán, N. A. Kotov, *Nano Lett.* **2010**, *10*, 4013 – 4019.
[23] R. Contreras-Cáceres, I. Pastoriza-Santos, R. A. Alvarez-Puebla, J. Pérez-Juste, A. Fernández-Barbero, L. M. Liz-Marzán, *Chem. Eur. J.* **2010**, *16*, 9462 – 9467.
[24] Y. Feng, Y. Wang, H. Wang, T. Chen, Y. Y. Tay, L. Yao, Q. Yan, S. Li, H. Chen, *Small* **2012**, *8*, 246 – 251.
[25] O. M. Bakr, B. H. Wunsch, F. Stellacci, *Chem. Mater.* **2006**, *18*, 3297 – 3301.
[26] E. Hao, R. C. Bailey, G. C. Schatz, J. T. Hupp, S. Li, *Nano Lett.* **2004**, *4*, 327 – 330.
[27] H. Wang, N. J. Halas, *Adv. Mater.* **2008**, *20*, 820 – 825.
[28] L. Rodríguez-Lorenzo, R. Álvarez-Puebla, I. Pastoriza-Santos, S. Mazzucco, O. Stéphan, M. Kociak, L. M. Liz-Marzán, F. J. García de Abajo, *J. Am. Chem. Soc.* **2009**, *131*, 4616 – 4618.
[29] N. C. Seeman, *Nature* **2003**, *421*, 427 – 431.
[30] D. Zhu, H. Pei, J. Chao, S. Su, A. Aldalbahi, M. Rahaman, L. Wang, L. Wang, W. Huang, C. H. Fan, X. Zuo, *Nanoscale* **2015**, *7*, 18671 – 18676.

[31] W. Zhao, W. Chiuman, J. C. F. Lam, S. A. McManus, W. Chen, Y. Cui, R. Pelton, M. A. Brook, Y. Li, *J. Am. Chem. Soc.* **2008**, *130*, 3610 – 3618.
[32] K. Saha, S. S. Agasti, C. Kim, X. Li, V. M. Rotello, *Chem. Rev.* **2012**, *112*, 2739 – 2779.
[33] N. L. Rosi, D. A. Giljohann, C. S. Thaxton, A. K. R. Lytton-Jean, M. S. Han, C. A. Mirkin, *Science* **2006**, *312*, 1027 – 1030.
[34] D.-K. Lim, K.-S. Jeon, H. M. Kim, J.-M. Nam, Y. D. Suh, *Nat. Mater.* **2010**, *9*, 60 – 67.
[35] J. Hu, P. C. Zheng, J. H. Jiang, G. L. Shen, R. Q. Yu, G. K. Liu, *Analyst* **2010**, *135*, 1084 – 1089.
[36] W. Wang, X. Ding, M. He, J. Wang, X. Lou, *Anal. Chem.* **2014**, *86*, 10186 – 10192.
[37] H. D. Hill, J. E. Millstone, M. J. Banholzer, C. A. Mirkin, *ACS Nano* **2009**, *3*, 418 – 424.
[38] K. B. Cederquist, C. D. Keating, *ACS Nano* **2009**, *3*, 256 – 260.
[39] T. Kang, S. M. Yoo, I. Yoon, S. Y. Lee, B. Kim, *Nano Lett.* **2010**, *10*, 1189 – 1193.
[40] S. Mariani, S. Scarano, J. Spadavecchia, M. Minunni, *Biosens. Bioelectron.* **2015**, *74*, 981 – 988.
[41] F. L. Gao, Z. Zhu, J. L. Lei, H. X. Ju, *Chem. Commun.* **2012**, *48*, 10603 – 10605.
[42] Z. Opdahl, D. Y. Petrovykh, H. Kimura-Suda, M. J. Tarlov, L. J. Whitman, *Proc. Natl. Acad. Sci. USA* **2007**, *104*, 9 – 14.
[43] H. Pei, F. Li, Y. Wan, M. Wei, H. Liu, Y. Su, N. Chen, Q. Huang, C. H. Fan, *J. Am. Chem. Soc.* **2012**, *134*, 11876 – 11879.
[44] A. Halperin, A. Buhot, E. B. Zhulina, *Biophys. J.* **2005**, *89*, 796 – 811.
[45] P. Senthil Kumar, I. Pastoriza-Santos, B. Rodríguez-González, F. J. García de Abajo, L. M. Liz-Marzán, *Nanotechnology* **2008**, *19*, 015606.
[46] Y. W. C. Cao, R. Jin, C. A. Mirkin, *Science* **2002**, *297*, 1536 – 1540.
[47] P. G. Vianna, D. Grasseschi, G. K. B. Costa, I. C. S. Carvalho, S. H. Domingues, J. Fontana, C. J. S. de Matos, *ACS Photonics* **2016**, *3*, 1027 – 1035.
[48] L. M. Demers, C. A. Mirkin, R. C. Mucic, R. A. Reynolds, R. L. Letsinger, R. Elghanian, G. Viswanadham, *Anal. Chem.* **2000**, *72*, 5535 – 5541.
[49] G. Lu, T. Z. Forbes, A. J. Haes, *Analyst* **2016**, *141*, 5137 – 5143.
[50] J. Theiss, P. Pavaskar, P. M. Echternach, R. E. Muller, S. B. Cronin, *Nano Lett.* **2010**, *10*, 2749 – 2754.
[51] W. Haiss, N. T. K. Thanh, J. Aveyard, D. G. Fernig, *Anal. Chem.* **2007**, *79*, 4215 – 4221.

Manuscript received: February 26, 2017
Accepted manuscript online: May 15, 2017
Version of record online: June 20, 2017